Electronic Supplementary Information

Wet-Chemistry Topotactic Synthesis of Bimetallic Iron-Nickel Sulfide Nanoarrays: An Advanced and Versatile Catalyst for Energy-Efficient Overall Water and Urea Electrolysis

Wenxin Zhu,[a] Zhihao Yue,[a] Wentao Zhang,[a] Na Hu,[b] Zhengtao Luo,[a] Meirong Ren,[a] Zhijie Xu,[a] Ziyi Wei,[a] Yourui Suo[b] and Jianlong Wang*[a]

[a] College of Food Science and Engineering, Northwest A&F University, Yangling 712100, Shaanxi, China.

[b] Qinghai Key Laboratory of Qinghai-Tibet Plateau Biological Resources, Northwest Institute of Plateau Biology, Chinese Academy of Sciences, Xining 810008, Qinghai, China.

*Corresponding author. E-mail: wanglong79@yahoo.com (Jianlong Wang)

Experimental

***Materials*:** Nickel nitrate hexahydrate [$Ni(NO_3)_2 \cdot 6H_2O$], iron (III) nitrate nonahydrate [$Fe(NO_3)_3 \cdot 9H_2O$], urea, ammonium fluoride (NH_4F), and sodium sulfide (Na_2S) were purchased from Aladdin Industrial Corporation (analytical grade). All of the chemicals in this study were used as received without further purification. Ni foam (0.5 mm, areal density of 320 g/cm^2) was obtained from the Suzhou Jia Shi De Foam Metal Co. Ltd. and cleaned through sonicating consecutively in 3 M HCl, ethanol, and deionized (DI) water (several mins each) prior to using as a substrate. The water used throughout all experiments was purified through a Millipore system.

***Preparation of Fe_x-Ni_3S_2/Ni Foam*:** In a typical synthesis, for $Fe_{11.1\%}$-Ni_3S_2/Ni foam, first, 2 mmol $Ni(NO_3)_2 \cdot 6H_2O$, 0.25 mmol $Fe(NO_3)_3 \cdot 6H_2O$, 10 mmol urea, and 4 mmol NH_4F were dissolved in 40 mL deionized water in a 50 mL beaker under magnetic stirring for 15 min. The mixed pellucid solution was then transferred to a 50 mL Teflon-lined stainless steel autoclave with a piece of well-pretreated Ni foam (2 × 3 cm^2). Next, the autoclave was sealed and maintained at 120 °C for 6 h in an electric oven. After the autoclave was cooled at room temperature, the NiFe LDH/Ni foam was taken out and washed with ethanol and DI water several times to remove unreacted residues. Afterwards, to obtain corresponding sulfide, 0.1 M Na_2S (40 mL) was transferred to a 50 mL autoclave with the above NiFe LDH/Ni foam. The autoclave was then sealed and maintained at 150 °C for 9 h. After cooling to room temperature, the $Fe_{11.1\%}$-Ni_3S_2 nanowall arrays on Ni foam ($Fe_{11.1\%}$-Ni_3S_2/Ni foam) was washed with ethanol and DI water several times, followed by drying at 60 °C in the vacuum oven. Similarly, $Fe_{9.0\%}$-Ni_3S_2/Ni foam and $Fe_{14.3\%}$-Ni_3S_2/Ni foam were prepared by only adjusting the amount of $Fe(NO_3)_3 \cdot 6H_2O$ to 0.2 mmol and 0.335 mmol, respectively. Of note, during hydrothermal process, a small portion of Ni from Ni foam might be dissolved and participate in the building of Fe_x-Ni_3S_2 nanoarrays on account of the decomposition of urea, accurate measurement of the catalyst loading on the Ni foam was thereby challenging.

***Characterizations*:** Scanning electron microscope (SEM) images, energy dispersive X-ray spectroscopy (EDX) and corresponding mapping data were collected on a Hitachi S-4800 field emission scanning electron microscope at an accelerating voltage of 10 kV. X-ray diffraction (XRD) test was performed using a Bruker D8 advanced diffractometer with Cu K_α radiation (40 kV, 40 mA). Transmission electron microscope (TEM) test was made on a

HITACHI H-8100 electron microscopy (Hitachi, Tokyo, Japan) with an accelerating voltage of 200 kV. X-ray photoelectron spectroscopy (XPS) measurement was carried out on an ESCALABMK II X-ray photoelectron spectrometer using Mg as the exciting source.

***Electrochemical Measurements*:** All the electrochemical measurements were studied in a standard three-electrode glass cell with an electrolyte solution of 1.0 M KOH connected to a CHI660E analyzer (CH Instruments, China) using $Fe_{11.1\%}$-Ni_3S_2/Ni foam or NiFe LDH/Ni foam or bare Ni foam as the working electrode, a graphite rod as the counter electrode and a mercury/mercury oxide electrode (MOE, Hg/HgO/OH^-) as the reference electrode. In water-splitting measurement, the MOE reference electrode was calibrated with respect to reversible hydrogen electrode (RHE), while in urea-electrolysis test, it was calibrated with respect to saturated calomel electrode (SCE). In 1.0 M KOH, E (RHE) = E (MOE) + 0.9254 V. In 1.0 M KOH + 0.33 M urea, E (SCE) = E (MOE) − 0.1426 V. The current densities in all tests were normalized to the geometrical area. *iR* compensation was performed after each test by the equation of $E_{corrected} = E_{uncorrected} - E_{correction} = E_{uncorrected} - iR$,[1] where E is the potential, i is the current flowing through the system, and R is the resistance. The value of R could be directly read out from the leftmost intersection between the Nyquist curve and X-axis at high frequencies.[1] In 1.0 M KOH, R = 2.84 Ω for $Fe_{11.1\%}$-Ni_3S_2/Ni foam, R = 2.91 Ω for NiFe LDH/Ni foam, and R = 3.22 Ω for Ni foam. Note that, all the electrochemical data tested in 1.0 M KOH with 0.33 M urea were recorded without *iR* compensation. Linear sweep voltammetrys (LSVs) were conducted in 1.0 M KOH with a relative-small scan rate of 2 mV s^{-1} to minimize the capacitive current. Tafel plots were recorded with the linear portions at low overpotentials fitted to the Tafel equation ($\eta = b \log j + a$, where η is the overpotential, j

is the current density, and *b* is the Tafel slope. Onset overpotentials were determined on account of the beginning of linear regime in the Tafel plot. Electrochemical impedance spectroscopy (EIS) tests were carried out in the frequency range of 100 kHz–0.005 Hz with a AC voltage amplitude of 5 mV. The measured impedance data were further fitted to a simplified Randles equivalent circuit to extract the charge transfer resistances. The two-electrode systems of full water splitting and overall urea electrolysis with $Fe_{11.1\%}$-Ni_3S_2/Ni foam as both the cathode and anode were powered by the CHI660E workstation or a 1.5 V battery or a 2.0 V solar cell in 1.0 M KOH without or with 0.33 M urea.

[1] Y. Shi and B. Zhang, *Chem. Soc. Rev.*, 2016, 45, 1529-1541.

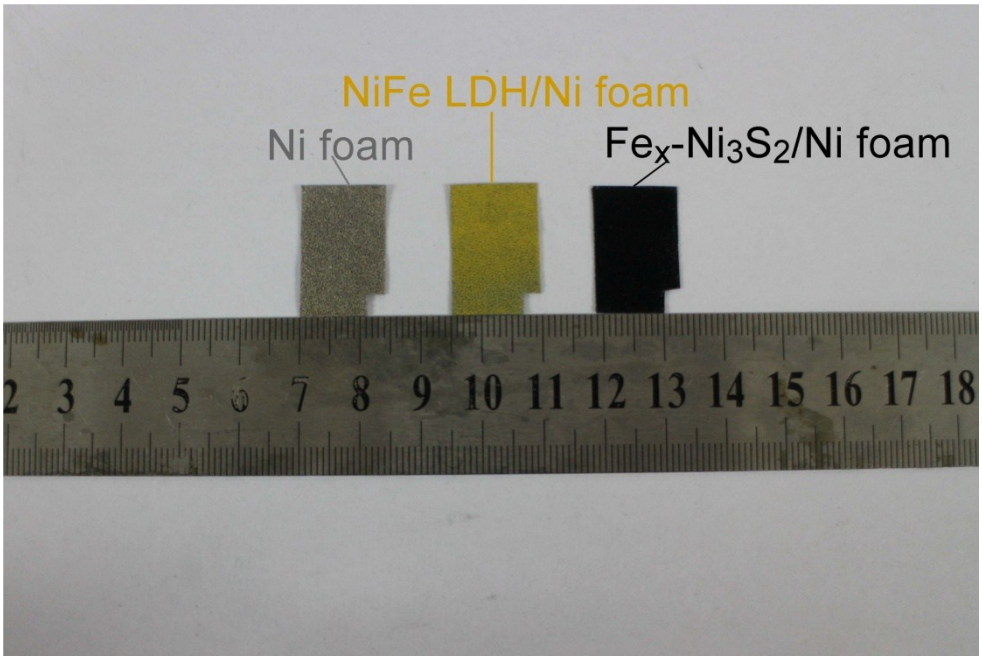

Fig. S1. Optical photographs of bare Ni foam (left), NiFe LDH/Ni foam (middle), and Fe_x-Ni_3S_2/Ni foam (right).

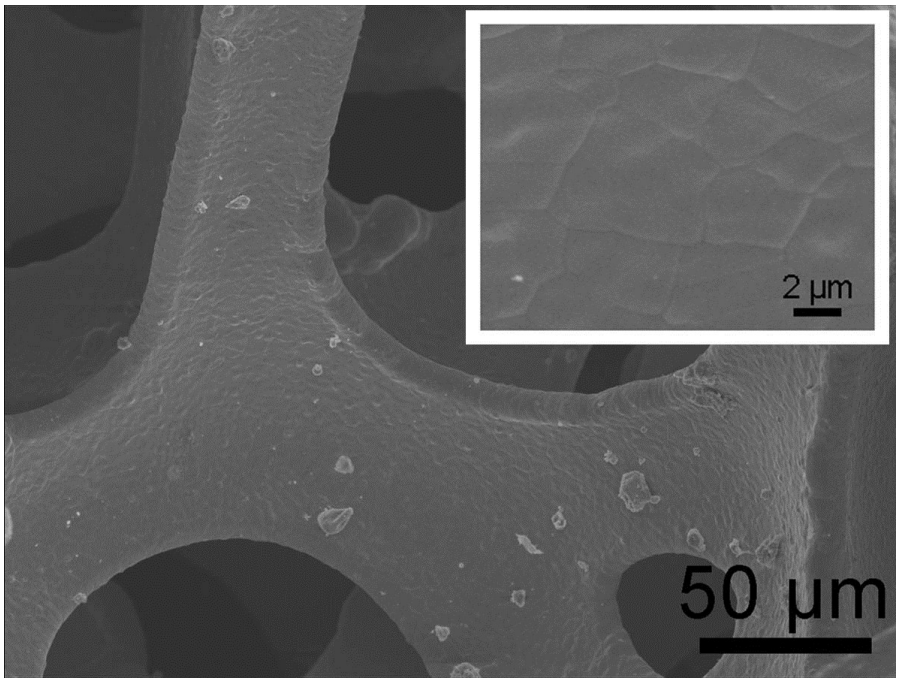

Fig. S2. Low- and high-magnification SEM images of bare Ni foam.

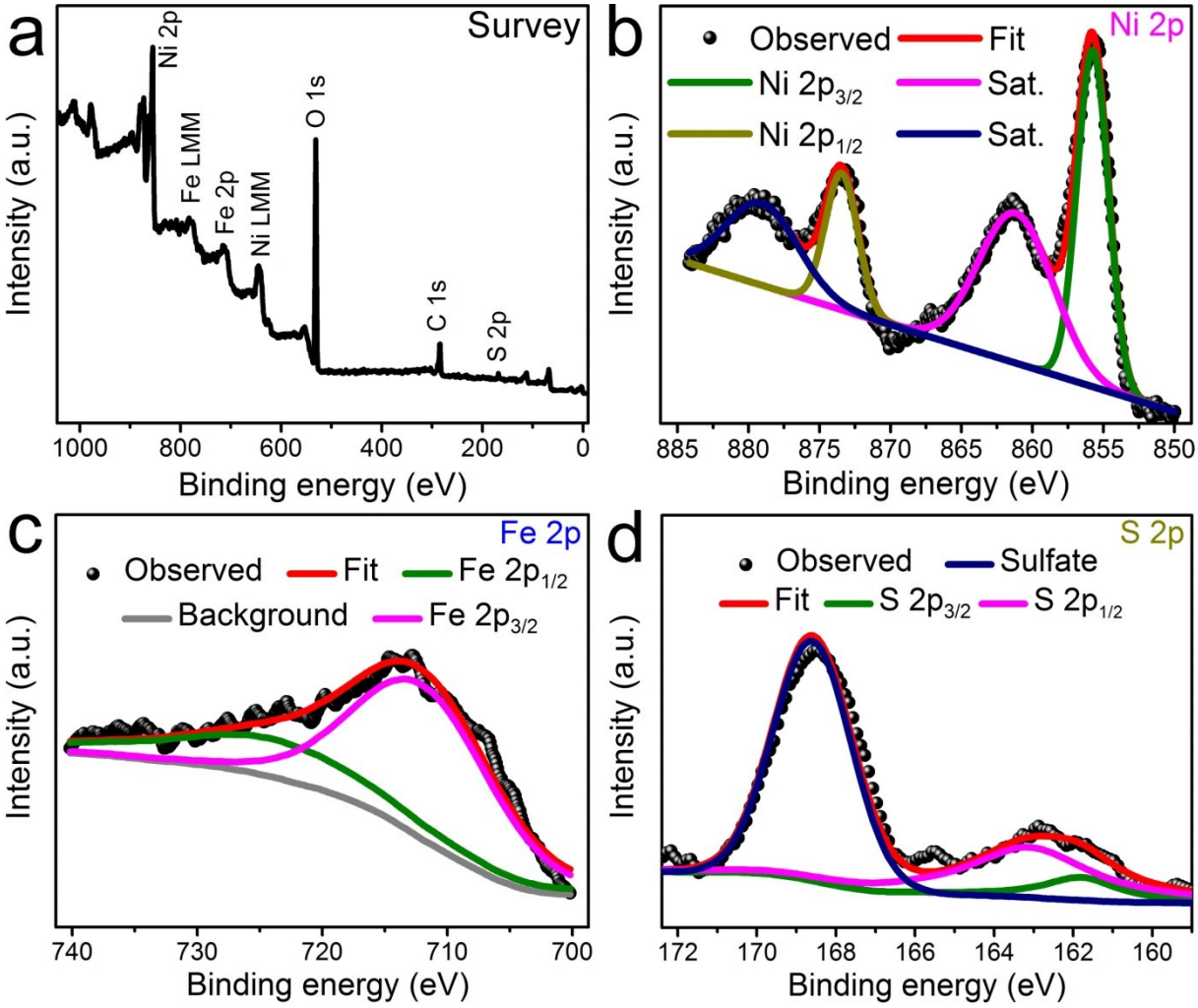

Fig. S3. XPS survey spectrum of $Fe_{11.1\%}$-Ni_3S_2/Ni foam. XPS spectra in the (b) Ni 2p, (c) Fe 2p, and (d) S 2p regions.

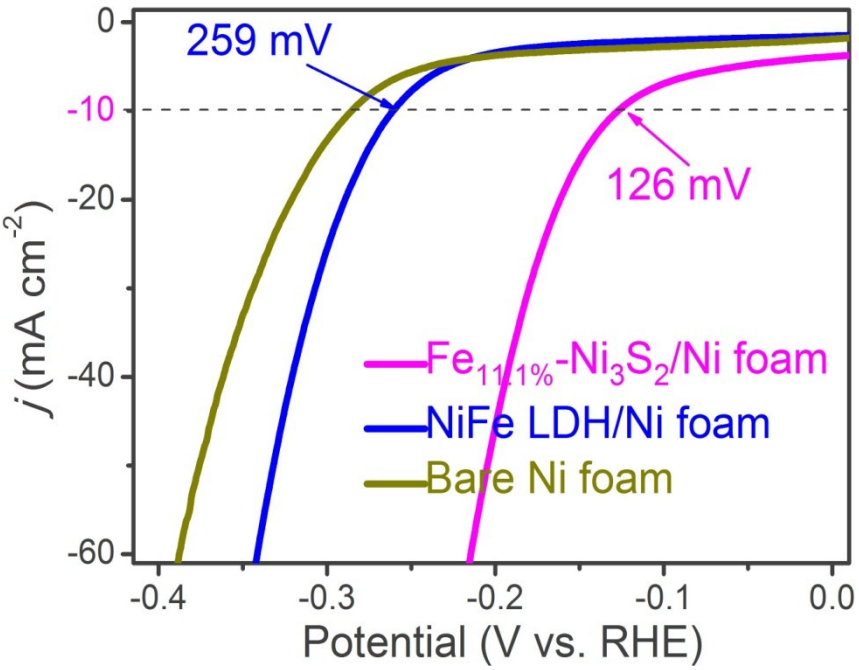

Fig. S4. Polarization curves of $Fe_{11.1\%}$-Ni_3S_2/Ni foam, NiFe LDH/Ni foam, and bare Ni foam for HER.

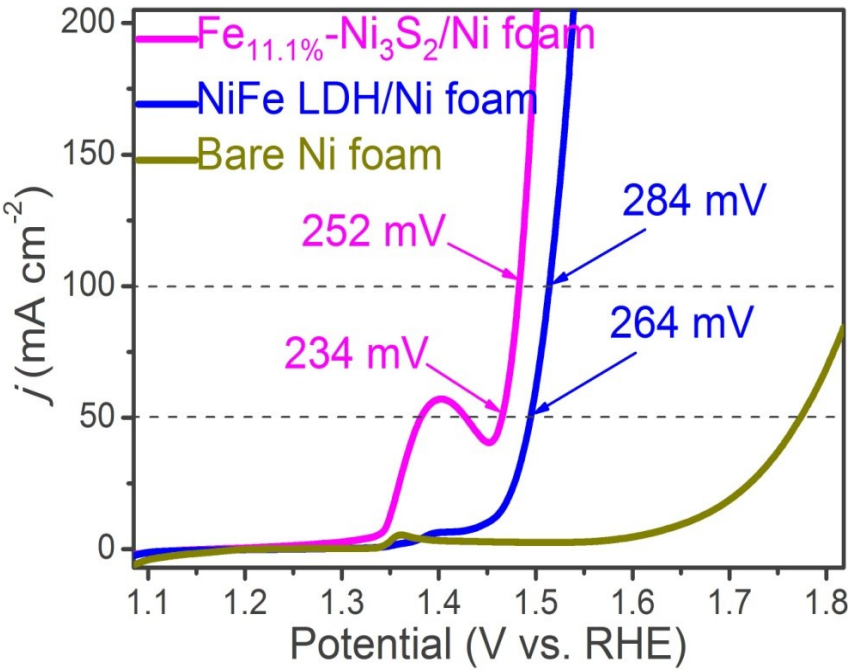

Fig. S5. Polarization curves of $Fe_{11.1\%}$-Ni_3S_2/Ni foam, NiFe LDH/Ni foam, and bare Ni foam for OER.

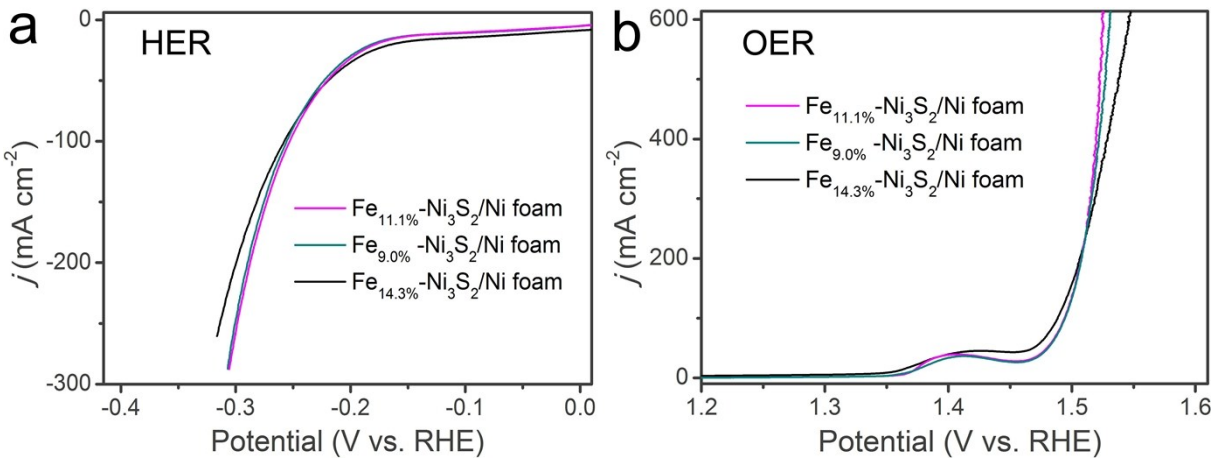

Fig. S6. Polarization curves of Fe_x-Ni_3S_2/Ni foam with different Fe contents of 9.0%, 11.1%, and 14.3% for HER and OER, respectively.

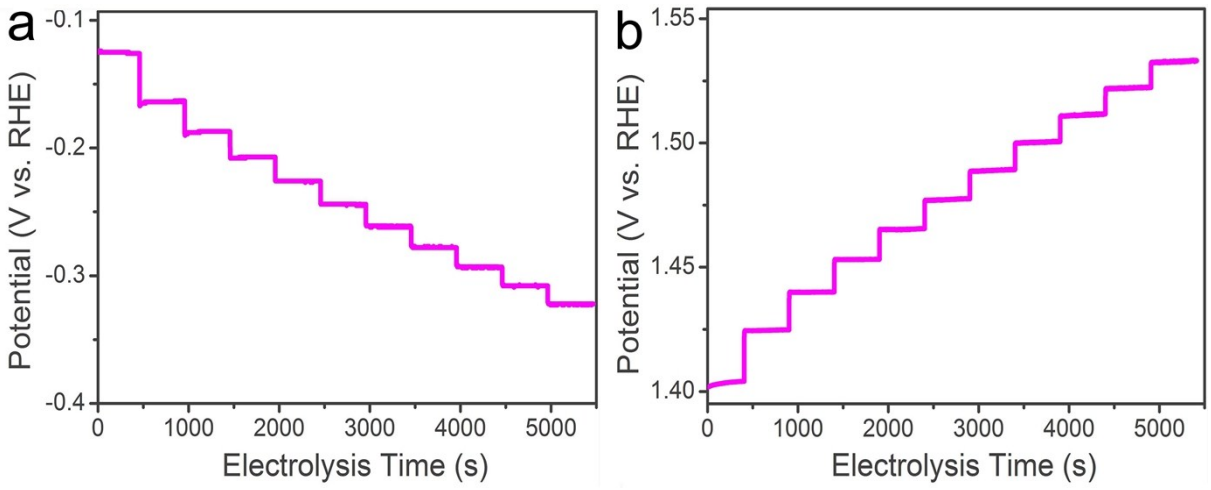

Fig. S7. Multi-current processes of $Fe_{11.1\%}$-Ni_3S_2/Ni foam for (a) HER and (b) OER. The current density started at ±10 mA cm^{-2} and ended at ±110 mA cm^{-2}, with an increment of ±10 mA cm^{-2} per 500 s without *iR* correction.

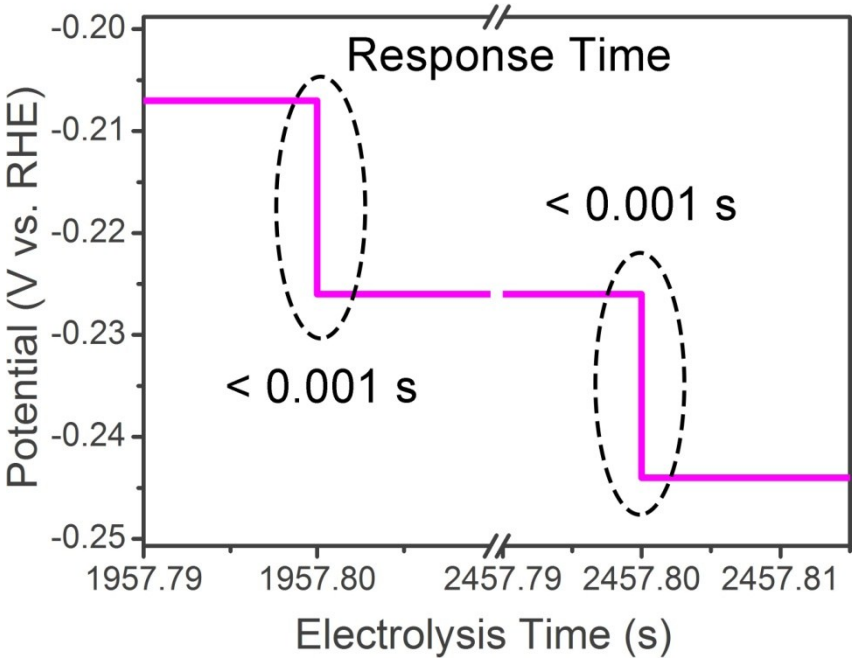

Fig. S8. The response time of current density changes from one step to another for HER.

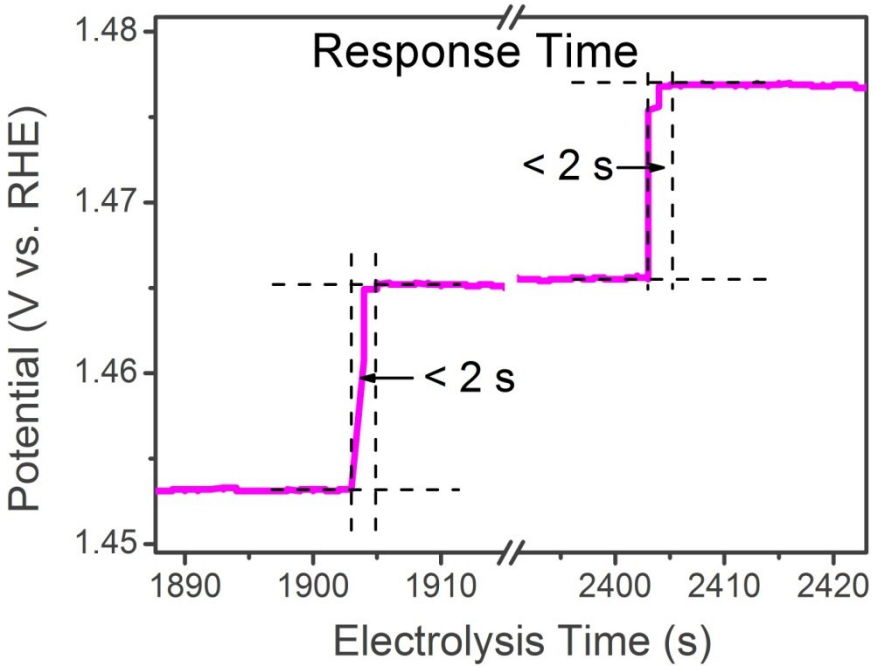

Fig. S9. The response time of current density changes from one step to another for OER.

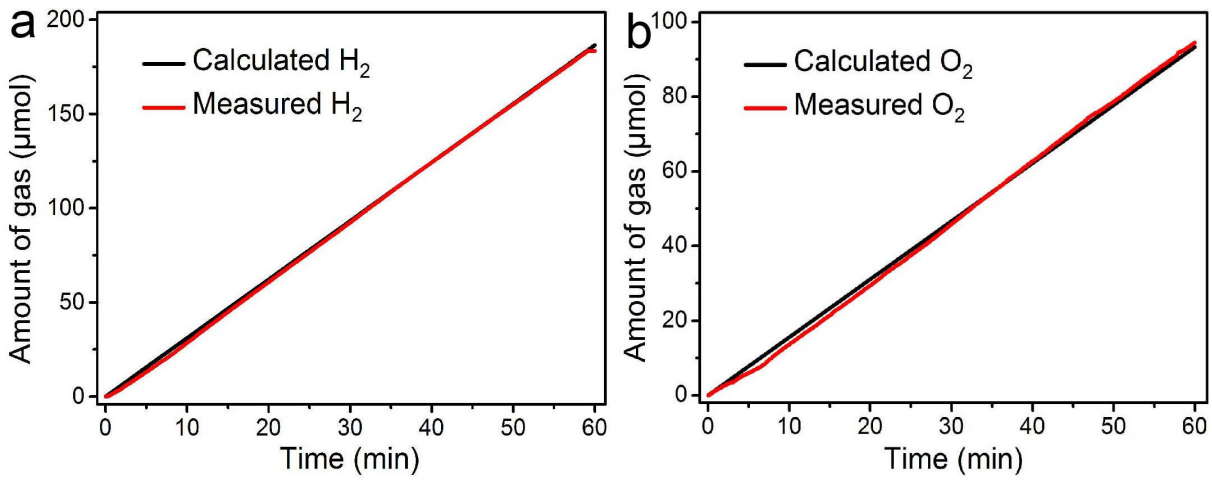

Fig. S10. The amount of evolved hydrogen and oxygen theoretically calculated and experimentally measured from $Fe_{11.1\%}$-Ni_3S_2/Ni foam *vs*. time for (a) HER and (b) OER in 1.0 M KOH, respectively.

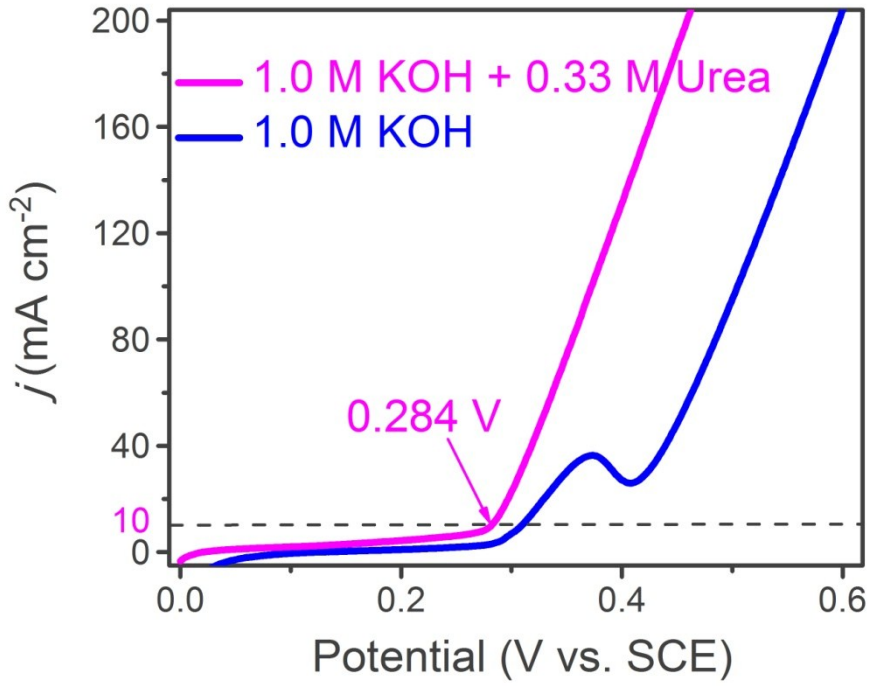

Fig. S11. Polarization curves of $Fe_{11.1\%}$-Ni_3S_2/Ni foam in 1.0 M KOH with and without 0.33 M urea with a scan rate of 2 mV s^{-1} for anodic oxidation reactions.

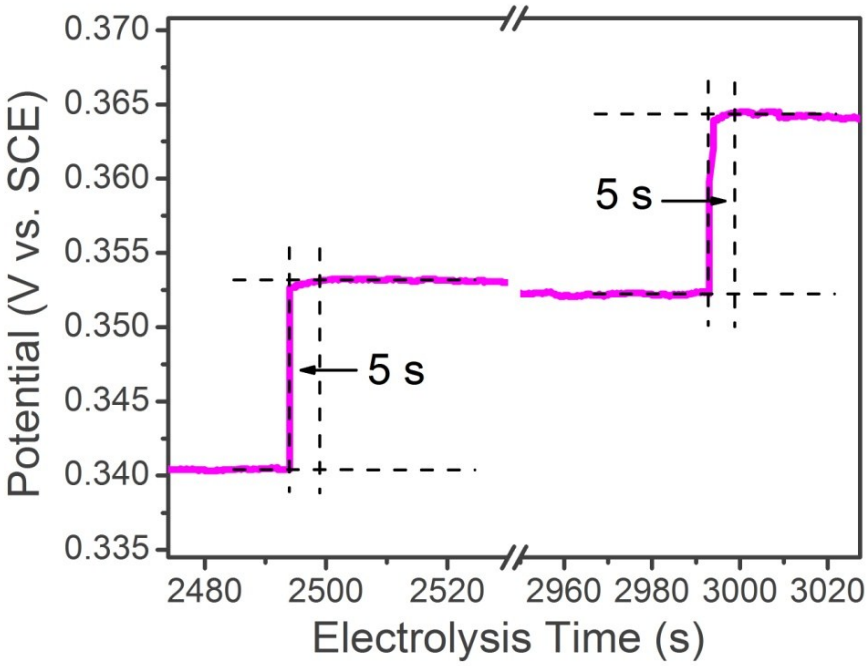

Fig. S12. The response time of current density changes from one step to another for UOR.

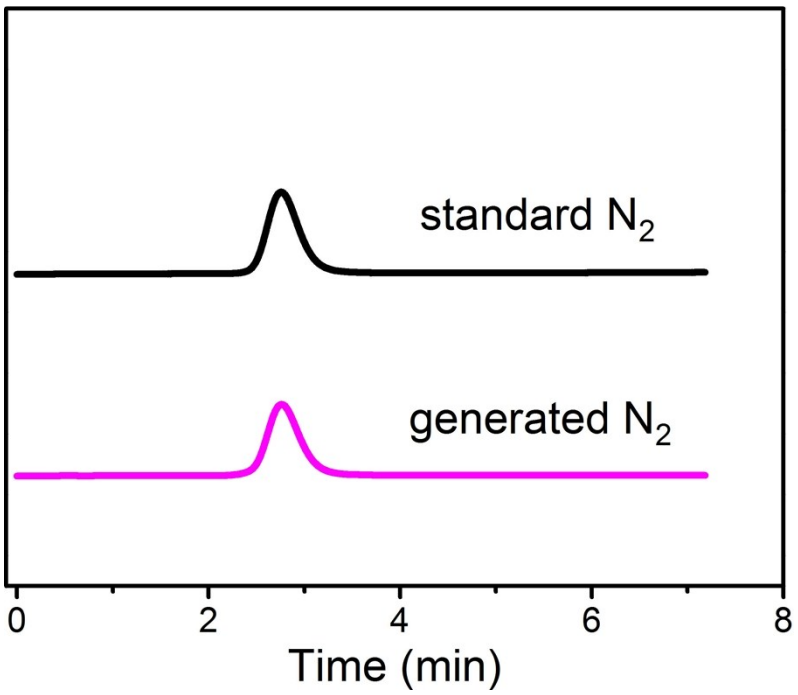

Fig. S13. Gas chromatography spectrum of N_2.

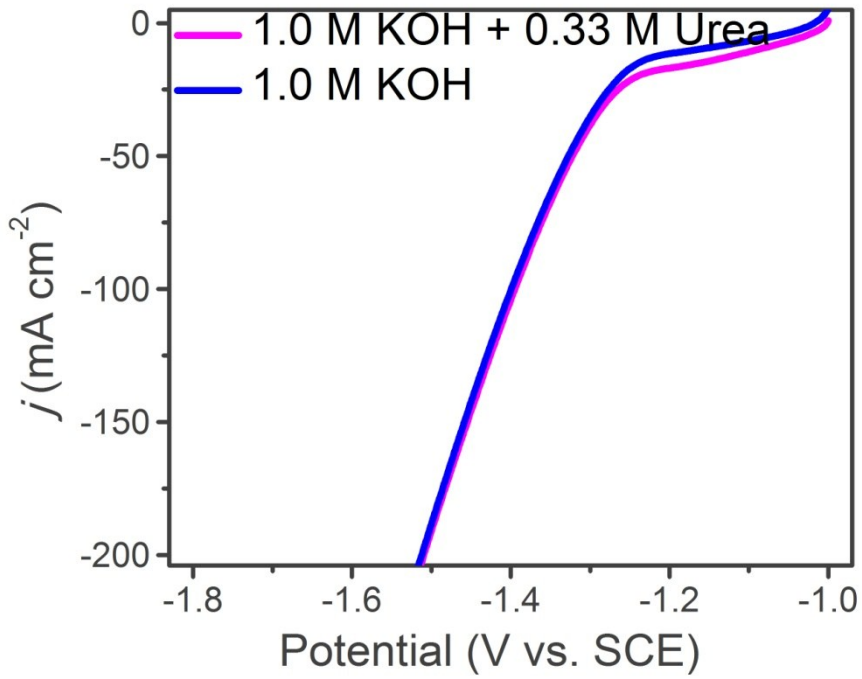

Fig. S14. Polarization curves of $Fe_{11.1\%}$-Ni_3S_2/Ni foam in 1.0 M KOH with and without 0.33 M urea with a scan rate of 2 mV s^{-1} for HER.

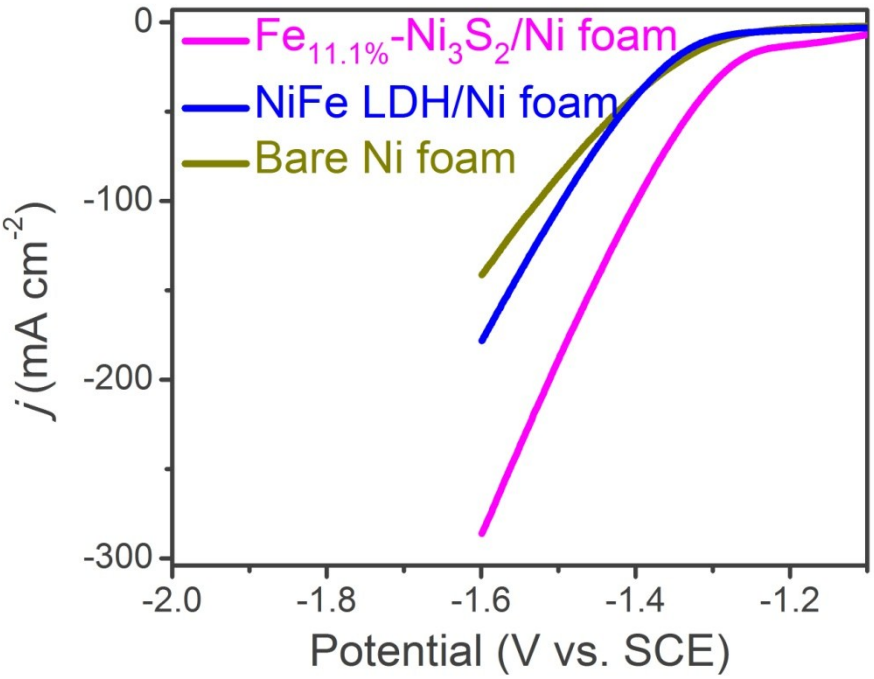

Fig. S15. Polarization curves of $Fe_{11.1\%}$-Ni_3S_2/Ni foam, NiFe LDH/Ni foam, and bare Ni foam in 1.0 M KOH with 0.33 M urea with a scan rate of 2 mV s^{-1} for HER.

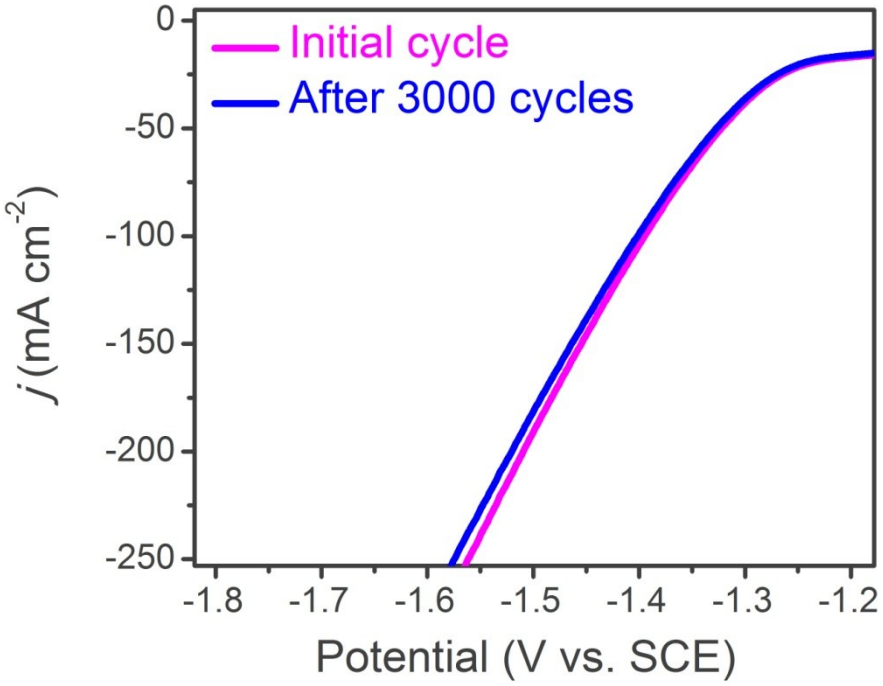

Fig. S16. LSV curves for $Fe_{11.1\%}$-Ni_3S_2/Ni foam before and after 3000 CV cycles for HER.

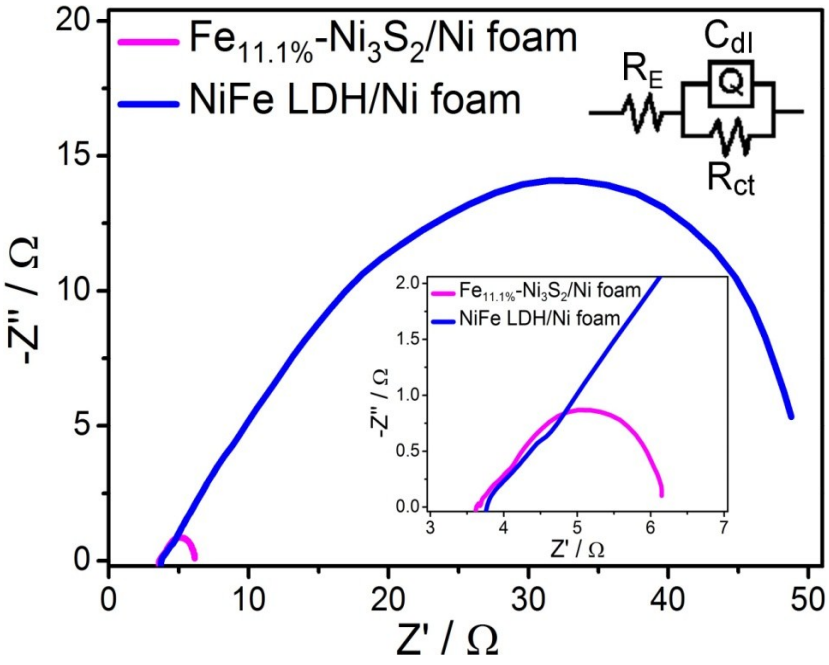

Fig. S17. Nyquist plots of $Fe_{11.1\%}$-Ni_3S_2/Ni foam and NiFe LDH/Ni foam in 1.0 M KOH recorded at 0.65 V *vs.* MOE under the influence of an AC voltage of 5 mV.

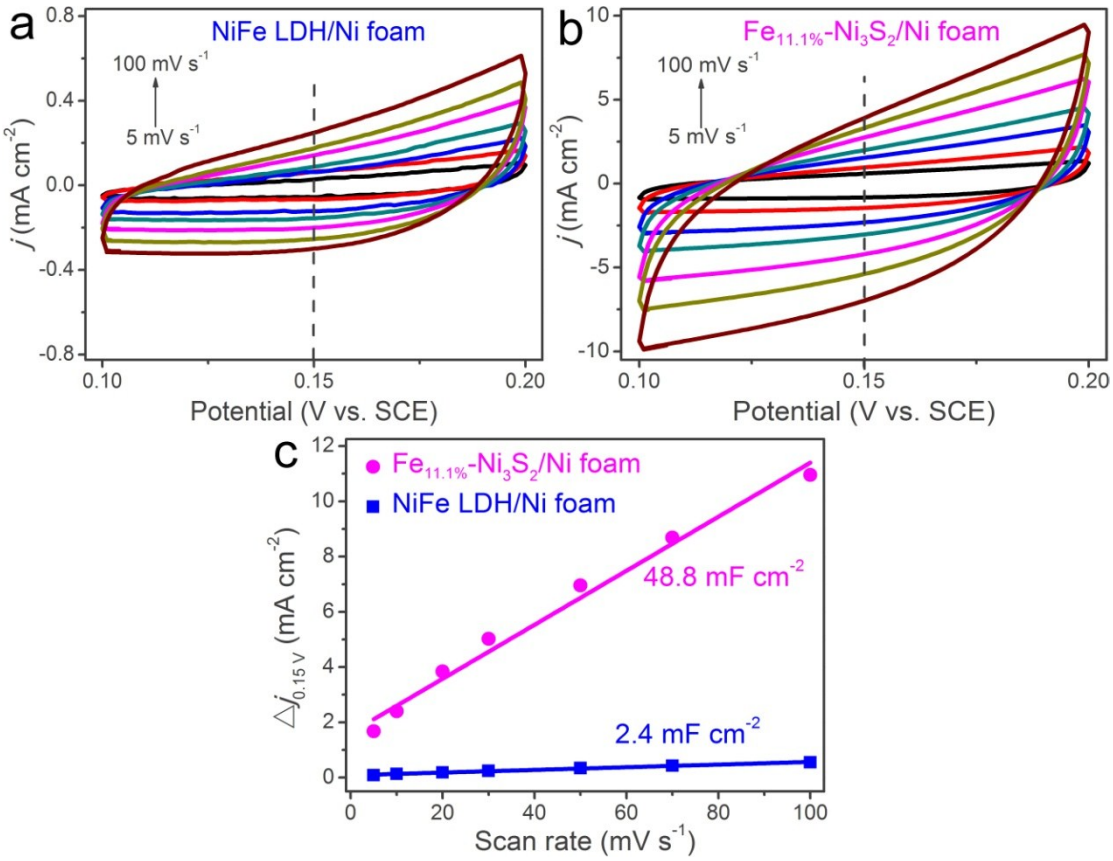

Fig. S18. Typical cyclic voltammograms of (a) $Fe_{11.1\%}$-Ni_3S_2/Ni foam and (b) NiFe LDH/Ni foam with various scan rates (5–100 mV s^{-1}) in the region of 0.1–0.2 V (*vs.* SCE). (c) The capacitive current density at 0.15 V (*vs.* SCE) as a function of scan rate for $Fe_{11.1\%}$-Ni_3S_2/Ni foam and NiFe LDH/Ni foam in 1.0 M KOH.

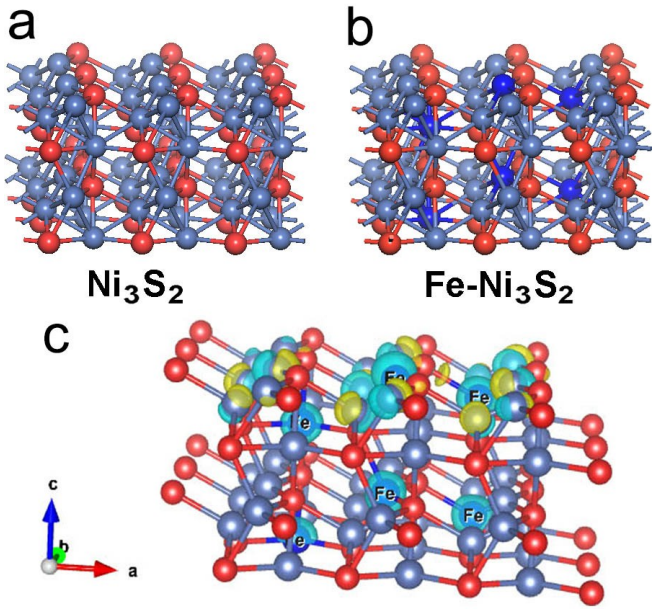

Fig. S19. Optimized structural representations of (a) Ni_3S_2 and (b) Fe-Ni_3S_2. (c) Calculated charge density differences of Fe-Ni_3S_2 interfaces. The Ni, Fe, and S atoms are marked in grey blue, dark blue, and orange, respectively. The light blue and yellow regions represent charge loss and charge accumulation, respectively. Charge density difference is obtained by subtracting the charge density of isolated Ni_3S_2 surface from that of Fe-Ni_3S_2 interfaces.

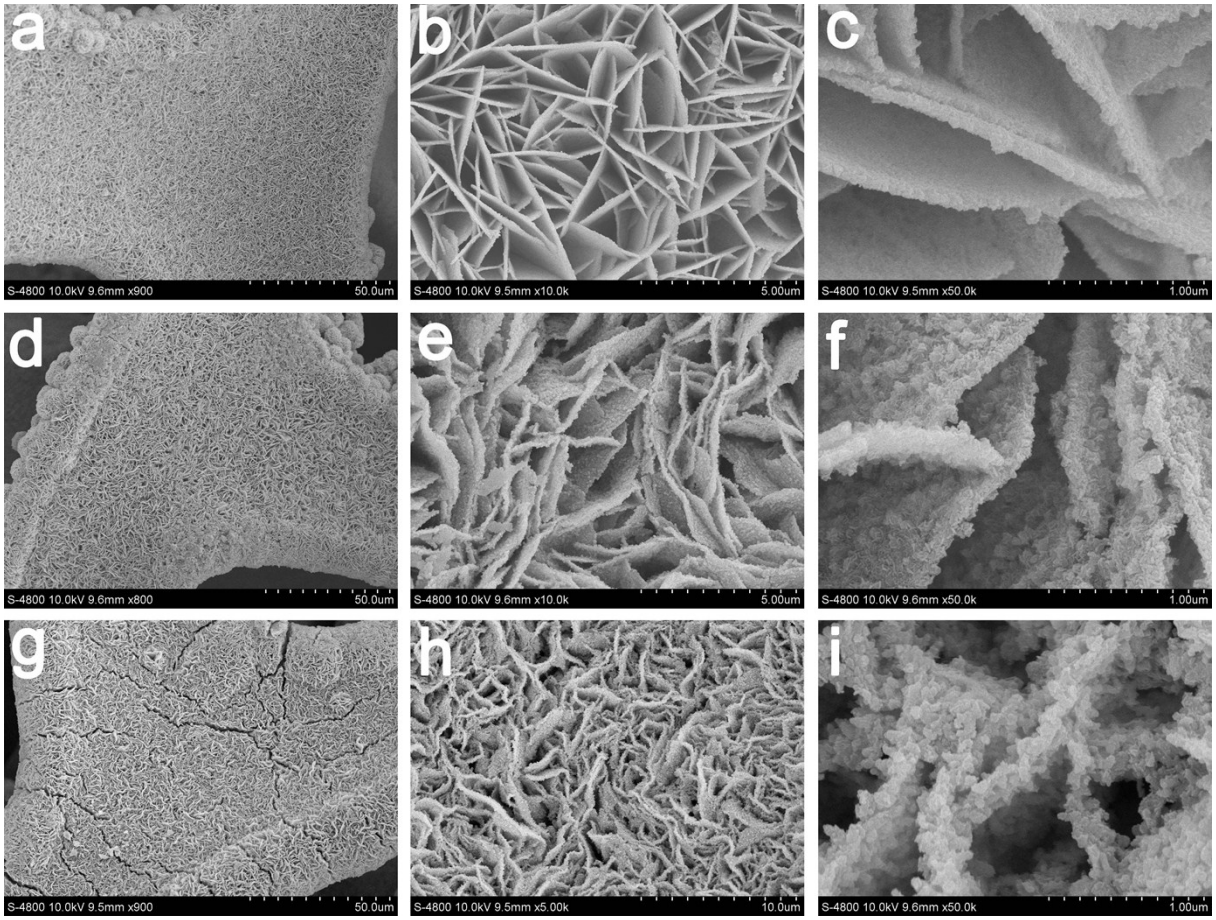

Fig. S20. SEM images of $Fe_{11.1\%}$-Ni_3S_2/Ni foam after long-term electrolysis for HER (a-c), OER (d-f), and UOR (g-i).

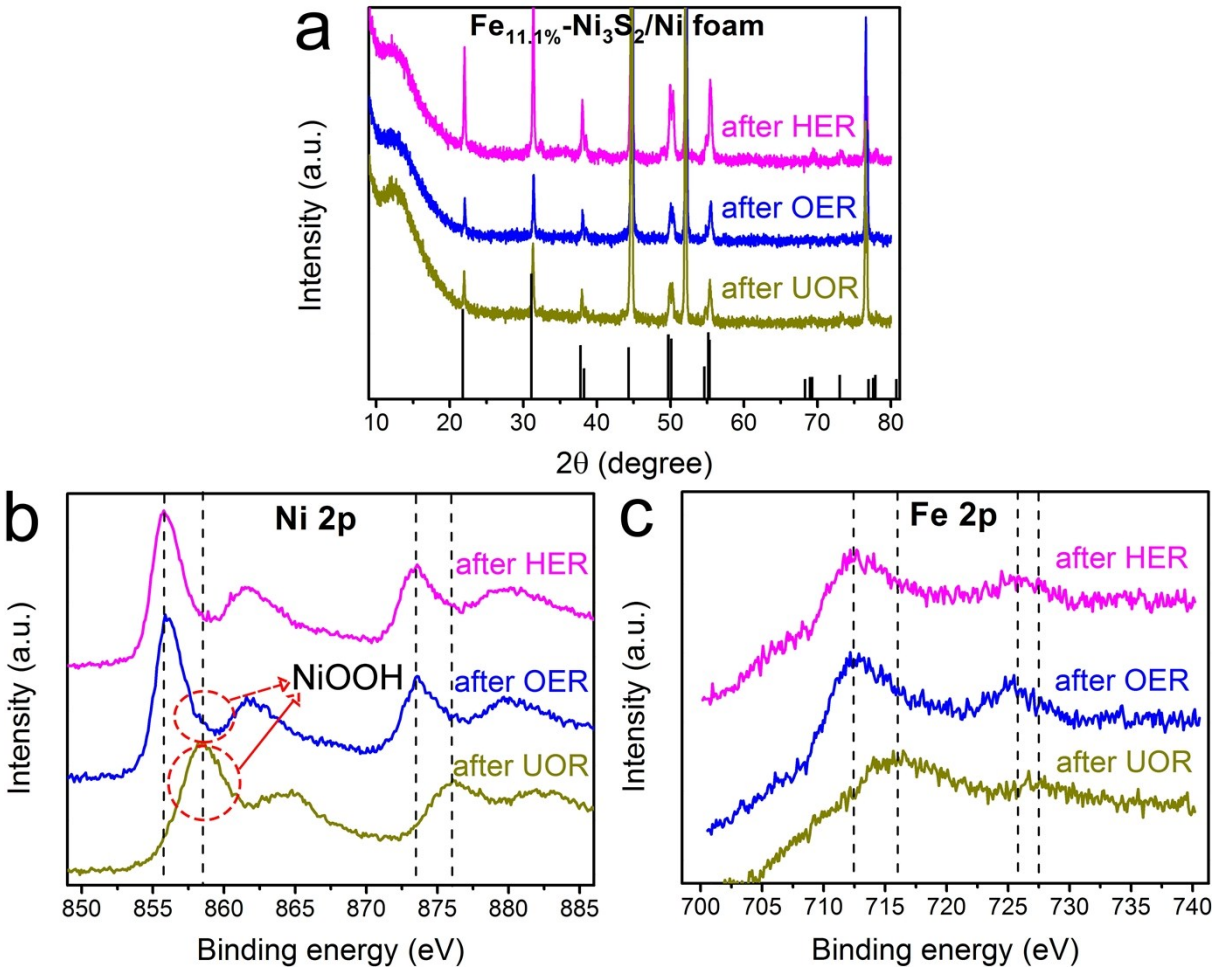

Fig. S21. XRD spectrum of $Fe_{11.1\%}$-Ni_3S_2/Ni foam after long-term electrolysis for HER, OER, and UOR. XPS spectra in Ni 2p and Fe 2p regions of $Fe_{11.1\%}$-Ni_3S_2/Ni foam after long-term electrolysis for HER, OER, and UOR.

Table S1. Comparison of HER performance in 1.0 M KOH for $Fe_{11.1\%}$-Ni_3S_2/Ni foam with other most-recently reported high-performance OER electrocatalysts.

Catalytic material	Current density ($mA\ cm^{-2}$)	Overpotential (mV)	Ref.
$Fe_{11.1\%}$-Ni_3S_2/Ni foam (array)	**10**	**126**	**This work**
	50	**203**	
NiFeS/Ni foam (film)	10	180	1
Ni_3S_2/Ni foam (array)	10	223	2
MoS_2/Carbon cloth (array)	50	~235	3
NiS/Ni foam (film)	50	~200	4
$NiCo_2S_4$/Carbon cloth (array)	50	~270	5
$NiCo_2S_4$/Ni foam (array)	10	210	6
CNTs@Co-S/Carbon paper (array)	10	190	7
Graphene-Ni_3Se_2@Co_9S_8	20	170	8
VOOH nanosphere	10	164	9
Co_1Mn_1CH/Ni foam (array)	10	200	10
CoP/Carbon cloth (array)	10	209	11
CoP/Ti foil (array)	10	128	12
Ni_2P/Carbon cloth (array)	10	~205	13
$FeNi_3N$/Ni foam (array)	10	202	14
Fe_2Ni_2N/Ni foam (array)	10	180	15

References

[1] P. Ganesan, A. Sivanantham and S. Shanmugam, *J. Mater. Chem. A*, 2016, **4**, 16394-16402.

[2] L. Feng, G. Yu, Y. Wu, G. Li, H. Li, Y. Sun, T. Asefa, W. Chen and X. Zou, *J. Am. Chem. Soc.*, 2015, **137**, 14023-14026.

[3] W. Zhu, C. Tang, D. Liu, J. Wang, A. M. Asiri and X. Sun, *J. Mater. Chem. A*, 2016, **4**, 7169-7173.

[4] W. Zhu, X. Yue, W. Zhang, S. Yu, Y. Zhang, J. Wang and J. Wang, *Chem. Commun.*, 2016, **52**, 1486-1489.

[5] D. Liu, Q. Lu, Y. Luo, X. Sun and A. M. Asiri, *Nanoscale*, 2015, **7**, 15122-15126.

[6] A. Sivanantham, P. Ganesan and S. Shanmugam, *Adv. Funct. Mater.*, 2016, **26**, 4661-4672.

[7] J. Wang, H. Zhong, Z. Wang, F. Meng and X. Zhang, *ACS Nano*, 2016, **10**, 2342-2348.

[8] Y. Hou, M. Qiu, G. Nam, M. G. Kim, T. Zhang, K. Liu, X. Zhuang, J. Cho, C. Yuan and X. Feng, *Nano Lett.*, 2017, **17**, 4202-4209.

[9] H. Shi, H. Liang, F. Ming and Z. Wang, *Angew. Chem.*, 2017, **129**, 588-592.

[10] T. Tang, W. Jiang, S. Niu, N. Liu, H. Luo, Y. Chen, S. Jin, F. Gao, L. Wan and J. Hu, *J. Am. Chem. Soc.*, 2017, **139**, 8320-8328.

[11] J. Tian, Q. Liu, A. M. Asiri and X. Sun, *J. Am. Chem. Soc.*, 2014, **136**, 7587-7590.

[12] C. Tang, R. Zhang, W. Lu, L. He, X. Jiang, A. M. Asiri and X. Sun, *Adv. Mater.*, 2017, **29**, 1602441.

[13] P. Jiang, Q. Liu and X. Sun, *Nanoscale*, 2014, **6**, 13440-13445.

[14] B. Zhang, C. Xiao, S. Xie, J. Liang, X. Chen and Y. Tang, *Chem. Mater.*, 2016, **28**, 6934-6941.

[15] M. Jiang, Y. Li, Z. Lu, X. Sun and X. Duan, *Inorg. Chem. Front.*, 2016, **3**, 630-634.

Table S2. Comparison of OER performance in 1.0 M KOH for $Fe_{11.1\%}$-Ni_3S_2/Ni foam with other most-recently reported high-performance OER electrocatalysts.

Catalytic material	Current density ($mA\ cm^{-2}$)	Overpotential (mV)	Ref.
$Fe_{11.1\%}$-Ni_3S_2/Ni foam (array)	**50**	**234**	**This work**
	100	**252**	
	500	**297**	
Fe-Ni_3S_2/FeNi foil (array)	10	282	1
Ni_3S_2/Ni foam (array)	10	260	2
CNTs@Co-S/Carbon paper (array)	10	306	3
Fe-NiO nanoparticle	10	297	4
Fe_2Ni_2N/Ni foam (array)	10	~240	5
$(Ni_{0.75}Fe_{0.25})Se_2$/CC (array)	100	277	6
Fe-CoP/Ti foil (array)	100	310	7
CoV_2O_6@V_2O_5/NRGO	10	239	8
$NiCo_2S_4$/Carbon cloth (array)	100	340	9
$NiCo_2S_4$/Ni foam (array)	10	260	10
Co_1Mn_1CH/Ni foam	30	294	11
Ni_3Se_2 film	10	290	12
NiSe/Ni foam (film)	20	270	13
$NiSe_2$/Ni foam (film)	20	295	14
Ni-P nanoplate	10	300	15
MoS_2/Co foam	10	270	16

CNTs@FeOOH/Carbon cloth	10	250	17
FeOOH@CeO_2/Ni foam	30	250	18
FeOOH@Co@FeOOH/Ni foam	100	310	19
VOOH nanosphere	10	270	20
NiS/Ni foam	50	335	21
MoS_2 microsphere/Ni foam	20	310	22
Ni-Co mixed oxide	10	380	23
$CoFe_2O_4$@C/Ni foam	10	240	24
Mn-Co oxyphosphide	10	320	25
CoAl LDH/graphene	10	252	26
Fe_xN/graphene/Ni foam	10	238	27
$Cu(OH)_2$@$CoCO_3(OH)_2$·nH_2O/Cu foam	100	290	28

References

[1] C. Yuan, Z. Sun, Y. Jiang, Z. Yang, N. Jiang, Z. Zhao, U. Y. Qazi, W. Zhang and A. Xu, *Small*, 2017, **13**, 1604161.

[2] L. Feng, G. Yu, Y. Wu, G. Li, H. Li, Y. Sun, T. Asefa, W. Chen and X. Zou, *J. Am. Chem. Soc.*, 2015, **137**, 14023-14026.

[3] J. Wang, H. Zhong, Z. Wang, F. Meng and X. Zhang, *ACS Nano*, 2016, **10**, 2342-2348.

[4] K. Fominykh, P. Chernev, I. Zaharieva, J. Sicklinger, G. Stefanic, M. Doblinger, A. Muller, A. Pokharel, S. Bocklein, C. Scheu, T. Bein and D. Fattakhova-Rohlfing, *ACS Nano*, 2015, **9**, 5180-5188.

[5] M. Jiang, Y. Li, Z. Lu, X. Sun and X. Duan, *Inorg. Chem. Front.*, 2016, **3**, 630-634.

[6] Z. Wang, J. Li, X. Tian, X. Wang, Y. Yu, K. A. Owusu, L. He and L. Mai, *ACS Appl. Mater. Interfaces*, 2016, **8**, 19386-19392.

[7] C. Tang, R. Zhang, W. Lu, L. He, X. Jiang, A. M. Asiri and X. Sun, *Adv. Mater.*, 2017, **29**, 1602441.

[8] F. Shen, Y. Wang, Y. Tang, S. Li, Y. Wang, L. Dong, Y. Li, Y. Xu and Y. Lan, *ACS Energy Lett.*, 2017, **2**, 1327-1333.

[9] D. Liu, Q. Lu, Y. Luo, X. Sun and A. M. Asiri, *Nanoscale*, 2015, **7**, 15122-15126.

[10] A. Sivanantham, P. Ganesan and S. Shanmugam, *Adv. Funct. Mater.*, 2016, **26**, 4661-4672.

[11] T. Tang, W. Jiang, S. Niu, N. Liu, H. Luo, Y. Chen, S. Jin, F. Gao, L. Wan and J. Hu, *J. Am. Chem. Soc.*, 2017, **139**, 8320-8328.

[12] A. T. Swesi, J. Masud and M. Nath, *Energy Environ. Sci.*, 2016, **9**, 1771-1782.

[13] C. Tang, N. Cheng, Z. Pu, W. Xing and X. Sun, *Angew. Chem. Int. Ed.*, 2015, **127**, 9483-9487.

[14] Z. Pu, Y. Luo, A. M. Asiri and X. Sun, *ACS Appl. Mater. Interfaces*, 2016, **8**, 4718-4723.

[15] X.-Y. Yu, Y. Feng, B. Guan, X. W. Lou and U. Paik, *Energy Environ. Sci.*, 2016, **9**, 1246-1250.

[16] D. Xiong, Q. Zhang, W. Li, J. Li, X. Fu, M. F. Cerqueira, P. Alpuim and L. Liu, *Nanoscale*, 2017, **9**, 2711-2717.

[17] Y. Zhang, G. Jia, H. Wang, B. Ouyang, R. S. Rawat and H. J. Fan, *Mater. Chem. Front.*, 2017, **1**, 709-715.

[18] J.-X. Feng, S.-H. Ye, H. Xu, Y.-X. Tong and G.-R. Li, *Adv. Mater.*, 2016, **28**, 4698-4703.

[19] J.-X. Feng, H. Xu, Y.-T. Dong, S.-H. Ye, Y.-X. Tong and G.-R. Li, *Angew. Chem.*, 2016, **55**, 3694-3698.

[20] H. Shi, H. Liang, F. Ming and Z. Wang, *Angew. Chem.*, 2017, **129**, 588-592.

[21] W. Zhu, X. Yue, W. Zhang, S. Yu, Y. Zhang, J. Wang and J. Wang, *Chem. Commun.*, 2016, **52**, 1486-1489.

[22] K. Yan and Y. Lu, *Small*, 2016, **12**, 2975-2981.

[23] L. Han, X.-Y. Yu and X. W. Lou, *Adv. Mater.*, 2016, **28**, 4601-4605.

[24] X.-F. Lu, L.-F. Gu, J.-W. Wang, J.-X. Wu, P.-Q. Liao and G.-R. Li, *Adv. Mater.*, 2017, **29**, 1604437.

[25] B. Y. Guan, L. Yu and X. W. Lou, *Angew. Chem. Int. Ed.*, 2017, **56**, 2386-2389.

[26] J. Ping, Y. Wang, Q. Lu, B. Chen, J. Chen, Y. Huang, Q. Ma, C. Tan, J. Yang, X. Cao, Z.

Wang, J. Wu, Y. Ying and H. Zhang, *Adv. Mater.*, 2016, **28**, 7640-7645.

[27] F. Yu, H. Zhou, Z. Zhu, J. Sun, R. He, J. Bao, S. Chen and Z. Ren, *ACS Catal.*, 2017, **7**, 2052-2057.

[28] L. Xie, C. Tang, K. Wang, G. Du, A. M. Asiri and X. Sun, *Small*, 2017, **13**, 1602755.

Table S3. Comparison of the overall electrolysis efficiency for $Fe_{11.1\%}$-Ni_3S_2/Ni foam in 1.0 M KOH with other most-recently reported high-performance bifunctional electrocatalysts.

Catalytic material	Voltage@10 mA cm^{-2}	Ref.
$Fe_{11.1\%}$-Ni_3S_2/Ni foam (array)	**1.60**	**This work**
NiSe/Ni foam	1.63	1
NiFe LDH/$Co_{0.85}Se$/EG	1.67	2
NiFe/$NiCo_2O_4$/Ni foam	1.67	3
Cu_3P/Ni foam	1.67	4
Ni-CoS_2/Carbon cloth	1.66	5
$NiSe_2$/Ti plate	1.66	6
NiS/Ni foam	1.64	7
Fe-CoP/Ti foil	1.60	8
Ni-P/Ni foam	1.64	9
Fe_2Ni_2N/Ni foam	1.65	10
NiCoP/Ni foam	1.58	11
Co_3Se_4/Co foam	1.59	12
CoP/Carbon cloth	1.65	13
$NiCo_2S_4$/Carbon cloth	1.68	14
$NiCo_2S_4$/Ni foam	1.63	15
Co_3O_4/Ni foam	1.63	16
Fe-Ni_2P/Ni foam	1.61	17
$MoNi_4$/Ni foam	1.58	18
VOOH/Ni foam	1.62	19
Ni_8P_3/Ni foam	1.61	20
CoP/Ni foam	1.62	21
WO_2/Ni foam	1.59	22
$FeNi_3N$/Ni foam	1.62	23

$Ni(OH)_2$/Ni foam	1.68	24

References

[1] C. Tang, N. Cheng, Z. Pu, W. Xing and X. Sun, *Angew. Chem. Int. Ed.*, 2015, **127**, 9483-9487.

[2] Y. Hou, M. R. Lohe, J. Zhang, S. Liu, X. Zhuang and X. Feng, *Energy Environ. Sci.*, 2016, **9**, 478-483.

[3] C. Xiao, Y. Li, X. Lu and C. Zhao, *Adv. Funct. Mater.*, 2016, **26**, 3515-3523.

[4] A. Han, H. Zhang, R. Yuan, H. Ji and P. Du, *ACS Appl. Mater. Interfaces*, 2017, **9**, 2240-2248.

[5] W. Fang, D. Liu, Q. Lu, X. Sun and A. M. Asiri, *Electrochem. Commun.*, 2016, **63**, 60-64.

[6] Z. Pu, Y. Luo, A. M. Asiri and X. Sun, *ACS Appl. Mater. Interfaces*, 2016, **8**, 4718-4723.

[7] W. Zhu, W. Zhang, S. Yu, Y. Zhang, J. Wang and J. Wang, *Chem. Commun.*, 2016, **52**, 1486-1489.

[8] C. Tang, R. Zhang, W. Lu, L. He, A. M. Asiri and X. Sun, *Adv. Mater.*, 2017, **29**, 1602441.

[9] X. Wang, W. Li, D. Xiong, D. Y. Petrovykh and L. Liu, *Adv. Funct. Mater.*, 2016, **26**, 4067-4077.

[10] M. Jiang, Y. Li, Z. Lu, X. Sun and X. Duan, *Inorg. Chem. Front.*, 2016, **3**, 630-634.

[11] H. Liang, A. N. Gandi, D. H. Anjum, X. Wang, U. Schwingenschlögl and H. N. Alshareef, *Nano Lett.*, 2016, **16**, 7718-7725.

[12] W. Li, X. Gao, D. Xiong, F. Wei, W. Song, J. Xu and L. Liu, *Adv. Energy Mater.*, 2017, **7**, 1602579.

[13] T. Liu, L. Xie, J. Yang, R. Kong, G. Du, A. M. Asiri, X. Sun and L. Chen, *ChemElectroChem*, 2017, **4**, 1840-1845.

[14] D. Liu, Q. Lu, Y. Luo, X. Sun and A. M. Asiri, *Nanoscale*, 2015, **7**, 15122-15126.

[15] A. Sivanantham, P. Ganesan and S. Shanmugam, *Adv. Funct. Mater.*, 2016, **26**, 4661-4672.

[16] Y. P. Zhu, T. Y. Ma, M. Jaroniec and S. Z. Qiao, *Angew. Chem. Int. Ed.*, 2017, **56**, 1324-1328.

[17] P. Wang, Z. Pu, Y. Li, L. Wu, Z. Tu, M. Jiang, Z. Kou, I. S. Amiinu and S. Mu, *ACS Appl. Mater. Interfaces*, 2017, **9**, 26001-26007.

[18] Y. Jin, X. Yue, C. Shu, S. Huang and P. K. Shen, *J. Mater. Chem. A*, 2017, **5**, 2508-2513.

[19] H. Shi, H. Liang, F. Ming and Z. Wang, *Angew. Chem.*, 2017, **129**, 588-592.

[20] G. Chen, T. Y. Ma, Z. Liu, Y. Su, K. Davey and S. Qiao, *Adv. Funct. Mater.*, 2016, **26**, 3314-3323.

[21] Y. Zhu, Y. Liu, T. Ren and Z. Yuan, *Adv. Funct. Mater.*, 2015, **25**, 7337-7347.

[22] C. Shu, S. Kang, Y. Jin, X. Yue and P. K. Shen, *J. Mater. Chem. A*, 2017, **5**, 9655-9660.

[23] B. Zhang, C. Xiao, S. Xie, J. Liang, X. Chen and Y. Tang, *Chem. Mater.*, 2016, **28**, 6934-6941.

[24] Y. Rao, Y. Wang, H. Ning, P. Li and M. Wu, *ACS Appl. Mater. Interfaces*, 2016, **8**, 33601-33607.

Table S4. Comparison of UOR performance in 1.0 M KOH with 0.33 or 0.5 M urea for $Fe_{11.1\%}$-Ni_3S_2/Ni foam with other most-recently reported superior UOR electrocatalysts.

Catalytic material	Urea concentration (M)	Current density (mA cm^{-2})	Potential (V *vs.* SCE)	Ref.
$Fe_{11.1\%}$-Ni_3S_2/Ni foam (array)	**0.33**	**10**	**0.284**	**This work**
		100	**0.372**	
Ni_3N/Carbon cloth (array)	0.33	100	0.462	1
Ni_2P/Carbon cloth (array)	0.5	100	0.447	2
$Ni(OH)_2$ nanosheets	0.33	10	0.452	3
MnO_2 nanosheets	0.5	100	~0.445	4
$Zn_{0.08}Co_{0.92}P$/Ti mesh (array)	0.5	50	~0.42	5
$NiMoO_4$/Ni foam (array)	0.33	10	~0.292	6
$Ni(OH)_2$ (array)	0.33	10	0.312	7
CE-NiFe/Ni foam (film)	0.33	10	0.302	8
NiO/Ni foam (array)	0.33	10	0.312	9
$Ni(OH)_2$/Ni foam (array)	0.33	10	0.342	10
CoS_2/Ti mesh (array)	0.3	10	0.332	11

References

[1] Q. Liu, L. Xie, F. Qu, Z. Liu, G. Du, A. M. Asiri and X. Sun, *Inorg. Chem. Front.*, 2017, **4**, 1120-1124.

[2] D. Liu, T. Liu, L. Zhang, F. Qu, G. Du, A. M. Asiri and X. Sun, *J. Mater. Chem. A*, 2017, **5**, 3208-3213.

[3] X. Zhu, X. Dou, J. Dai, X. An, Y. Guo, L. Zhang, S. Tao, J. Zhao, W. Chu, X. C. Zeng, C. Wu and Y. Xie, *Angew. Chem. Int. Ed.*, 2016, **55**, 12465-12469.

[4] S. Chen, J. Duan, A. Vasileff and S. Z. Qiao, *Angew. Chem. Int. Ed.*, 2016, **55**, 3804-3808.

[5] T. Liu, D. Liu, F. Qu, D. Wang, L. Zhang, R. Ge, S. Hao, Y. Ma, G. Du, A. M. Asiri, L. Chen and X. Sun, *Adv. Energy Mater.*, 2017, **7**, 1700020.

[6] Y. Liang, Q. Liu, A. M. Asiri and X. Sun, *Electrochim. Acta*, 2015, **153**, 456-460.

[7] M. Wu, R. Ji and Y. Zheng, *Electrochim. Acta*, 2014, **144**, 194-199.

[8] M. Wu, C. Jiao, F. Chuang and F. Chen, *Electrochim. Acta*, 2017, **227**, 210-216.

[9] M. Wu, G. Lin and R. Yang, *J. Power Sources*, 2014, **272**, 711-718.

[10] R. Ji, D. Chan, J. Jow and M. Wu, *Electrochem. Commun.*, 2013, **29**, 21-24.

[11] S. Wei, X. Wang, J. Wang, X. Sun, L. Cui, W. Yang, Y. Zheng and J. Liu, *Electrochim. Acta*, 2017, **246**, 776-782.